

Position Optimization for Two-layer Movable Antenna Systems

Liuja Yao, *Student Member, IEEE*, Changsheng You, *Member, IEEE*, Chao Zhou, *Student Member, IEEE*, Beixiong Zheng, *Senior Member, IEEE*, and Weidong Mei, *Member, IEEE*

Abstract—Movable antenna (MA) is a promising technology for improving the performance of wireless communication systems by providing new degrees-of-freedom (DoFs) in antenna position optimization. However, existing works on MA systems have mostly considered element-wise *single-layer* MA (SL-MA) arrays, where all the MAs move within the given movable region, hence inevitably incurring high control complexity and hardware cost in practice. To address this issue, we propose in this letter a new *two-layer* MA array (TL-MA), where the positions of MAs are jointly determined by the *large-scale movement* of multiple subarrays and the *small-scale fine-tuning* of per-subarray MAs. In particular, an optimization problem is formulated to maximize the sum-rate of the TL-MA-aided communication system by jointly optimizing the subarray-positions, per-subarray (relative) MA positions, and receive beamforming. To solve this non-convex problem, we propose an alternating optimization (AO)-based particle swarm optimization (PSO) algorithm, which alternately optimizes the positions of subarrays and per-subarray MAs, given the optimal receive beamforming. Numerical results verify that the proposed TL-MA significantly reduces the *sum-displacement* of MA motors (i.e., the total moving distances of all motors) of element-wise SL-MA, while achieving comparable rate performance.

Index Terms—Movable antenna (MA), position optimization, particle swarm optimization (PSO).

I. INTRODUCTION

With the wide deployment of the fifth-generation (5G) mobile communication networks, the next-generation wireless networks are expected to deliver orders-of-magnitude improvement in terms of network capacity, reliability, and latency reduction [1]. To this end, a variety of new antenna technologies have been recently proposed, e.g., fluid antenna systems (FAS) [2], (6D) movable antennas (MA) [3], [4], rotatable antennas (RA) [5], and pinching antenna systems (PASS) [6]. Unlike the existing multiple-input multiple-output (MIMO) systems based on fixed-position antennas (FPA), these position/rotation-agile antenna technologies provide an additional spatial degrees-of-freedom (DoFs) by dynamically adjusting the positions/rotations of antennas within a predefined region, thereby achieving better rate performance than conventional FPA systems [7].

Among others, MA technology has attracted growing research attention owing to its capability to provide flexible antenna position adjustment adaptive to dynamic environment.

L. Yao, C. You, and C. Zhou are with the Department of Electrical and Electronic Engineering, Southern University of Science and Technology, Shenzhen, China (e-mail: yaolj2024@mail.sustech.edu.cn; zhouchao2024@mail.sustech.edu.cn; youcs@sustech.edu.cn).

B. Zheng is with the School of Microelectronics, South China University of Technology, Guangzhou, China (e-mail: bxzheng@scut.edu.cn).

W. Mei is with the National Key Laboratory of Wireless Communications, University of Electronic Science and Technology of China, Chengdu, China (e-mail: wmei@uestc.edu.cn).

(Corresponding author: Changsheng You)

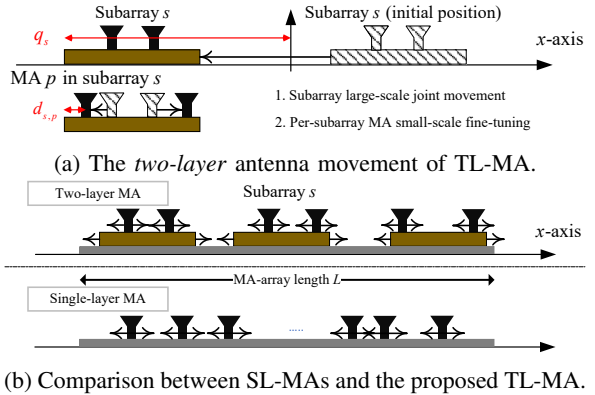


Fig. 1: Illustration of the proposed TL-MA and its comparison with conventional SL-MA.

ments. For example, the authors in [8] characterized the capacity of MA-aided MIMO systems for the single-user scenario, which was then extended to the multi-user MIMO scenario in [9]. While the performance gains of MAs have been verified in [8], [9], most existing works considered element-wise single-layer MA (SL-MA) architectures, as illustrated in Fig. 1(b). Such designs, however, may incur high hardware cost and implementation complexity in practice, since each MA element needs to be attached with a high-speed actuator (e.g., 10–20 m/s [10]) and their position optimization requires sophisticated path planning accounting for collision avoidance [10].

To achieve a more favorable trade-off between rate performance and hardware complexity, we propose in this letter a new *two-layer* MA (TL-MA) architecture as shown in Fig. 1(b). Specifically, this architecture employs a hierarchical positioning adjustment mechanism, where the positions of all MAs are jointly determined by the *large-scale movement* of subarrays as well as *small-scale fine-tuning* of per-subarray MAs. Specifically, we formulate an optimization problem to maximize the system sum-rate by jointly designing the positions of subarrays and MAs given the optimal receive beamforming. This high-dimensional non-convex problem is then solved by an efficient alternating optimization (AO)-based particle swarm optimization (PSO) algorithm. Numerical results show that the proposed TL-MA achieves comparable rate performance with SL-MA, yet requiring significantly smaller sum-displacement (and thus lower complexity). Moreover, the proposed AO-based PSO algorithm achieves better rate performance over the benchmark under the all-at-once antenna position optimization. In addition, it is worth noting that, compared to the existing array-wise MA architecture that adjusts the positions of subarrays only [11], our proposed TL-MA architecture also

incorporates small-scale fine-tuning of per-subarray antennas, thus achieving better rate performance.

II. SYSTEM MODEL AND PROBLEM FORMULATION

We consider a narrow-band multi-user MIMO system, where a new TL-MA is employed at the base station (BS) to serve K single-antenna users in the uplink under a quasi-static fading channel.

A. System Model

TL-MA Model: The proposed TL-MA array shown in Fig. 1(b) consists of $M = M_S \times M_A$ MAs in total, which are grouped into M_S movable subarrays (denoted as $\mathcal{M}_S \triangleq \{1, \dots, M_S\}$), each comprising M_A MAs (denoted as $\mathcal{M}_A \triangleq \{1, \dots, M_A\}$). As such, the positions of M MAs are jointly determined by the *large-scale* movement of subarrays and the *small-scale* fine-tuning of per-subarray MAs, as shown in Fig. 1(a). Specifically, the M_S subarrays have the same array length of L_A and can move flexibly in a prescribed movable region of length L (named as MA-array length, see Fig. 1(b)). The position of the s -th subarray, with $s \in \mathcal{M}_S$, can be determined by parameters $\{L_A, q_s\}$, where q_s denotes the x -axis coordinate of the starting point of the subarray s . Moreover, for subarray s , its MAs can adjust their positions in the interval $[q_s, q_s + L_A]$ at the x -axis. In addition, for the a -th ($a \in \mathcal{M}_A$) MA of subarray s , we denote by $d_{s,a}$ its *relative* distance from q_s (i.e., the starting point of its subarray). Then, its (absolute) position on the x -axis, denoted by $\delta_{s,a}$, is given by $\delta_{s,a} = q_s + d_{s,a}$. By defining $\mathbf{d}_s \triangleq \{d_{s,a}\}_{a=1}^{M_A} \in \mathbb{R}^{M_A \times 1}$, $\mathbf{q} \triangleq \{q_s\}_{s=1}^{M_S} \in \mathbb{R}^{M_S \times 1}$, $\boldsymbol{\delta}_s \triangleq [\delta_{s,1}, \dots, \delta_{s,M_A}]^T \in \mathbb{R}^{M_A \times 1}$, and $\boldsymbol{\delta} \triangleq [\boldsymbol{\delta}_1^T, \dots, \boldsymbol{\delta}_{M_S}^T]^T \in \mathbb{R}^{M \times 1}$, we obtain

$$\delta(\mathbf{q}, \{\mathbf{d}_s\}) = (\mathbf{q} \otimes \mathbf{1}_{M_A}) + [\mathbf{d}_1^T, \dots, \mathbf{d}_{M_S}^T]^T. \quad (1)$$

Unlike SL-MA which directly moves all MAs, TL-MA first moves subarrays (i.e., \mathbf{q}) and then fine-tunes MAs (i.e., $\{\mathbf{d}_s\}$), reducing implementation complexity (see Fig. 1). For the TL-MA movement, the following constraints need to be satisfied: First, to prevent the subarrays from overlapping with each other or exceeding the movable regions, we have

$$q_{s+1} - q_s \geq L_A, \quad \forall s = 1, 2, \dots, M_S - 1, \quad (2a)$$

$$-\frac{L}{2} \leq q_s \leq \frac{L}{2} - L_A, \quad \forall s = 1, 2, \dots, M_S. \quad (2b)$$

On the other hand, for each subarray s , the relative MA positions are constrained to prevent MAs from moving out of their subarray region and to ensure a minimum half-wavelength spacing, which are given by

$$\frac{\lambda}{4} \leq d_{s,a} \leq L_A - \frac{\lambda}{4}, \quad \forall a = 1, 2, \dots, M_A, \forall s, \quad (3a)$$

$$d_{s,a+1} - d_{s,a} \geq \frac{\lambda}{2}, \quad \forall a = 1, 2, \dots, M_A - 1, \forall s. \quad (3b)$$

Channel Model: Let $\mathbf{h}_k(\mathbf{q}, \{\mathbf{d}_s\}) \in \mathbb{C}^{M \times 1}, \forall k \in \mathcal{K}$ denote the channel from user k to the TL-MA array with $\mathcal{K} \triangleq \{1, \dots, K\}$, which is assumed to be perfectly known¹

¹The existing MA channel estimation methods (see, e.g., [7]) can be applied to acquire the channel state information (CSI). For the case with imperfect CSI, robust beamforming methods can be applied to guarantee the worst-case performance [12], which is left for our future work.

at the BS. Specifically, the channel \mathbf{h}_k is modeled as

$$\mathbf{h}_k^H(\mathbf{q}, \{\mathbf{d}_s\}) = \sum_{n=1}^{N_{PA}} \beta_{k,n} \mathbf{b}^H(\theta_{k,n}, \mathbf{q}, \{\mathbf{d}_s\}), \quad (4)$$

where $\beta_{k,n}$ is the complex-valued channel gain of the n -th path for user k , N_{PA} is the number of paths, and $\theta_{k,n}$ is the spatial angle between the n -th scatterer of user k and the MA-array. Herein, $\mathbf{b}(\theta_{k,n}, \mathbf{q}, \{\mathbf{d}_s\}) \in \mathbb{C}^{M \times 1}$ denotes the far-field channel steering vector, which is given by

$$\mathbf{b}(\theta_{k,n}, \mathbf{q}, \{\mathbf{d}_s\}) = [e^{-j\frac{2\pi}{\lambda}\delta_1\theta_{k,n}}, \dots, e^{-j\frac{2\pi}{\lambda}\delta_M\theta_{k,n}}]^T, \quad (5)$$

where λ is the carrier wavelength and $\boldsymbol{\delta}_m \triangleq [\boldsymbol{\delta}]_m$.

Signal Model: Let x_k denote the data symbol transmitted by user k , which satisfies $\mathbb{E}[x_k^H x_k] = P_t, \forall k \in \mathcal{K}$, with P_t representing its transmit power. As such, the received signal at the BS can be expressed as

$$\mathbf{y} = \mathbf{Hx} + \mathbf{z}, \quad (6)$$

where $\mathbf{H} = [\mathbf{h}_1(\mathbf{q}, \{\mathbf{d}_s\}), \dots, \mathbf{h}_K(\mathbf{q}, \{\mathbf{d}_s\})] \in \mathbb{C}^{M \times K}$ is the channel matrix, $\mathbf{x} = [x_1, \dots, x_K]^T \in \mathbb{C}^{K \times 1}$ is the transmit signal vector, and $\mathbf{z} \sim \mathcal{CN}(0, \sigma^2 \mathbf{I})$ is the received additive white Gaussian noise (AWGN) vector at the BS. To decode the uplink signal of each user k , the receive beamforming vector $\mathbf{v}_k \in \mathbb{C}^{M \times 1}$ is applied at the BS with $\|\mathbf{v}_k\|^2 = 1$. As such, the decoded signal from the k -th user is given by

$$\hat{x}_k = \mathbf{v}_k^H \mathbf{y} = \mathbf{v}_k^H \mathbf{h}_k x_k + \mathbf{v}_k^H \sum_{i \neq k}^K \mathbf{h}_i x_i + \mathbf{v}_k^H \mathbf{z}, \quad \forall k \in \mathcal{K}, \quad (7)$$

and its achievable rate in bits/second/Hertz (bps/Hz) is

$$R_k(\mathbf{q}, \{\mathbf{d}_s\}, \{\mathbf{v}_k\}) = \log_2 \left(1 + \frac{\gamma |\mathbf{v}_k^H \mathbf{h}_k|^2}{\gamma \sum_{i \neq k}^K |\mathbf{v}_k^H \mathbf{h}_i|^2 + 1} \right), \quad (8)$$

where $\gamma = \frac{P_t}{\sigma^2}$ is the transmit signal-to-noise ratio (SNR).

Displacement model: To evaluate the implementation complexity of different MA hardware architectures, we consider a new metric called *sum-displacement*, which characterizes the total moving distances of all MA motors, and represents one of the main metrics of the system cost (e.g., hardware cost, movement control complexity, energy consumption) [10], [11]. Specifically, for the proposed TL-MA, its sum-displacement of all subarrays is $C_S = \sum_s |q_s^{(0)} - q_s^*|$, where $q_s^{(0)}$ (or q_s^*) are the initial (or optimized) positions of the subarrays, respectively. In addition, the sum-displacement of all MAs in movement fine-tuning is $C_A = \sum_s \sum_a |d_{s,a}^{(0)} - d_{s,a}^*|$, where $d_{s,a}^{(0)}$ (or $d_{s,a}^*$) are the initial (or optimized) relative positions of the MAs in subarray s , respectively.

B. Problem Formulation

We aim to maximize the uplink sum-rate² by jointly optimizing the subarray-positions \mathbf{q} , the per-subarray *relative* MA-positions $\{\mathbf{d}_s\}$, and the receive beamforming $\{\mathbf{v}_k\}$.

²This work focuses on the uplink sum-rate maximization problem under the given TL-MA architecture (i.e., the number of subarrays and per-subarray length). For the more general objective that balances sum-rate with the associated sum-displacement cost, the problem can be formulated as a multi-objective optimization problem. The Pareto-optimal solutions can be obtained via exhaustive search, the details of which are left for future work.

This optimization problem can be formulated as

$$(P1) \quad \max_{\mathbf{q}, \{\mathbf{d}_s\}, \{\mathbf{v}_k\}} \sum_{k=1}^K R_k(\mathbf{q}, \{\mathbf{d}_s\}, \{\mathbf{v}_k\}) \quad (9a)$$

$$\text{s.t.} \quad (2a), (2b), (3a), (3b), \\ \|\mathbf{v}_k\|^2 = 1, \forall k \in \mathcal{K}, \quad (9b)$$

where (9b) is the unit-power constraint for receive beamforming. Problem (P1) is generally hard to solve optimally due to its non-concave objective function and non-convex constraints. Moreover, the coupled two-layer position optimization variables (i.e., \mathbf{q} and $\{\mathbf{d}_s\}$) make problem (P1) even more challenging, rendering existing MA-position optimization methods, such as successive convex approximation (SCA) [8] and PSO [9], much less effective.

III. PROPOSED SOLUTION TO PROBLEM (P1)

In this section, we propose an efficient algorithm to solve the sum-rate maximization problem (P1). Specifically, given arbitrary subarray positions \mathbf{q} and relative MA positions $\{\mathbf{d}_s\}$, we first obtain the optimal receive beamforming $\{\mathbf{v}_k\}$ in closed form, based on which the original problem (P1) is reformulated as an equivalent problem for optimizing \mathbf{q} and $\{\mathbf{d}_s\}$. Then we further develop an AO-based algorithm to iteratively optimize these two-layer position variables until the convergence is achieved.

A. Optimization of Receive Beamforming

Given any subarray-positions \mathbf{q} and relative MA-positions $\{\mathbf{d}_s\}$, problem (P1) reduces to optimizing the receive beamforming only for maximizing the signal-to-interference-plus-noise ratio (SINR) of each user k , which is given by

$$\text{SINR}_k = \frac{\gamma \mathbf{h}_k^H \mathbf{v}_k|^2}{\gamma \sum_{i \neq k}^K |\mathbf{h}_i^H \mathbf{v}_k|^2 + 1} = \frac{\gamma \mathbf{v}_k^H \mathbf{h}_k \mathbf{h}_k^H \mathbf{v}_k}{\mathbf{v}_k^H \mathbf{C}_k \mathbf{v}_k}, \forall k \in \mathcal{K}, \quad (10)$$

with $\mathbf{C}_k \triangleq \gamma \sum_{i \neq k}^K \mathbf{h}_i \mathbf{h}_i^H + \mathbf{I}$ being the interference-plus-noise covariance matrix for user k . By employing minimum mean square error (MMSE) receive beamforming [11], the maximum SINR for user k can be obtained, whose MMSE receive beamforming is

$$\mathbf{v}_k^* = \underset{\|\mathbf{v}_k\|^2=1}{\operatorname{argmax}} \frac{\gamma \mathbf{v}_k^H \mathbf{h}_k \mathbf{h}_k^H \mathbf{v}_k}{\mathbf{v}_k^H \mathbf{C}_k \mathbf{v}_k} = \frac{\mathbf{C}_k^{-1} \mathbf{h}_k}{\|\mathbf{C}_k^{-1} \mathbf{h}_k\|}, \forall k \in \mathcal{K}. \quad (11)$$

B. Joint Position Optimization of Subarrays and Antennas

By substituting the optimal receive beamforming $\{\mathbf{v}_k^*\}$ into (11), the original problem (P1) can be reformulated as the following problem for optimizing the subarray-positions \mathbf{q} and relative MA-positions $\{\mathbf{d}_s\}$ (named as MA-positions in the sequel for brevity)

$$(P2) \quad \max_{\mathbf{q}, \{\mathbf{d}_s\}} \tilde{R}(\mathbf{q}, \{\mathbf{d}_s\}) \quad (12a)$$

$$\text{s.t.} \quad (2a), (2b), (3a), (3b),$$

where $\tilde{R}(\mathbf{q}, \{\mathbf{d}_s\}) \triangleq \sum_{k=1}^K R_k(\mathbf{q}, \{\mathbf{d}_s\}, \{\mathbf{v}_k^*\})$ is the sum-rate under the optimal receive beamforming. However, problem (P2) is still a non-convex problem and hard to solve optimally due to the non-concave objective function (12a). The high dimensionality of the optimization variables $(\mathbf{q}, \{\mathbf{d}_s\})$

also makes this problem even more challenging. To tackle these difficulties, we propose an efficient AO-based PSO algorithm to solve problem (P2). Specifically, it alternately optimizes the subarray-positions \mathbf{q} and per-subarray MA-positions $\{\mathbf{d}_s\}$ with the other being fixed, until the convergence is achieved, whose details are presented below.

1) *Optimization of Subarray-Positions*: Given any MA-positions $\{\mathbf{d}_s\}$, problem (P2) reduces to the following problem for optimizing the subarray-positions \mathbf{q}

$$(P3) \quad \max_{\mathbf{q}} \tilde{R}(\mathbf{q}, \{\mathbf{d}_s\}) \quad \text{s.t.} \quad (2a), (2b).$$

Problem (P3) is challenging to solve optimally because of the non-concave objective function $\tilde{R}(\mathbf{q}, \{\mathbf{d}_s\})$. To address this issue, the PSO algorithm is employed to obtain a high-quality solution to problem (P3), with the details for updating subarray-positions \mathbf{q} presented below [9].

Initialization: At the beginning of the PSO algorithm, a swarm of I_P (whose index set is $\mathcal{I}_P \triangleq \{1, 2, \dots, I_P\}$) feasible position vectors are generated. The position of particle i is denoted by $\mathbf{q}_i^{(0)} \in \mathbb{R}^{M_S \times 1}$, $i \in \mathcal{I}_P$, with $\mathbf{s}_i^{(0)} \in \mathbb{R}^{M_S \times 1}$, $i \in \mathcal{I}_P$ denoting its initial speed, which is adjusted to search for high-quality subarray-positions.

Fitness Function Design: To evaluate the quality of any subarray-position \mathbf{q} , the following fitness function is considered [9]

$$\mathcal{F}_S(\mathbf{q}) = \tilde{R}(\mathbf{q}, \{\mathbf{d}_s\}) - \kappa P_S(\mathbf{q}), \quad (13)$$

where the first term corresponds to the objective function in problem (P3) and the second term is the subarray-wise penalty function accounting for constraints (2a) and (2b). Specifically, κ is the penalty coefficient and $P_S(\mathbf{q})$ is

$$P_S(\mathbf{q}) = \sum_{s=1}^{M_S-1} [L_A - (q_{s+1} - q_s)]^+ + \sum_{s=1}^{M_S} \left(\left[-\frac{L}{2} - q_s \right]^+ \left[q_s - \left(\frac{L}{2} - L_A \right) \right]^+ \right), \quad (14)$$

where $[x]^+ \triangleq \max(0, x)$. Note that the first and second terms in (14) respectively characterize the extent of violation for constraints (2a) and (2b) for subarray positions \mathbf{q} .

Positions Update: Let t denote the PSO iteration index, with $\mathcal{T} \triangleq \{1, 2, \dots, t\}$. In each PSO iteration, the update of the position is determined by the personal-best position of particle i (among its personal history) from the previous iteration, denoted by $\mathbf{q}_{i,pbest}^{(t-1)} \in \mathbb{R}^{M_S \times 1}$, and the global-best position (among the particle swarm) from the previous iteration, denoted by $\mathbf{q}_{gbest}^{(t-1)} \in \mathbb{R}^{M_S \times 1}$. Specifically, the personal/global-best positions are respectively given by

$$\mathbf{q}_{i,pbest}^{(t-1)} = \underset{\tau \in \mathcal{T} \setminus \{t\}}{\operatorname{argmax}} \mathcal{F}_S(\mathbf{q}_i^{(\tau)}), \forall i \in \mathcal{I}_P, \quad (15a)$$

$$\mathbf{q}_{gbest}^{(t-1)} = \underset{i \in \mathcal{I}_P}{\operatorname{argmax}} \mathcal{F}_S(\mathbf{q}_{i,pbest}^{(t-1)}). \quad (15b)$$

Given the obtained personal-best and global-best positions, the speed of the i -th particle is updated as follows

$$\mathbf{s}_i^{(t)} = \omega \mathbf{s}_i^{(t-1)} + c_1 \mathbf{r}_1^{(t-1)} \odot (\mathbf{q}_{i,pbest}^{(t-1)} - \mathbf{q}_i^{(t-1)}) + c_2 \mathbf{r}_2^{(t-1)} \odot (\mathbf{q}_{gbest}^{(t-1)} - \mathbf{q}_i^{(t-1)}), \forall i \in \mathcal{I}_P, \quad (16)$$

where $\mathbf{r}_1^{(t-1)}, \mathbf{r}_2^{(t-1)} \in \mathbb{R}^{M_S \times 1}$ are element-wise uniform random vectors sampled from $\mathcal{U}(0, 1)$ to promote swarm diversity, ω is the inertia coefficient, and c_1, c_2 are the personal and global learning coefficients, respectively [9]. Finally, with the updated speed $\mathbf{s}_i^{(t)}$, the position of the i -th particle is updated as

$$\mathbf{q}_i^{(t)} = \mathbf{q}_i^{(t-1)} + \mathbf{s}_i^{(t)}, \forall i \in \mathcal{I}_P. \quad (17)$$

By updating candidate subarray-positions in each PSO iteration following the procedures in (16)–(17), a suboptimal solution to problem (P3), denoted by \mathbf{q}^* , is obtained after I_T PSO iterations.

2) *Optimization of Antenna-Positions*: For ease of exposition, we define $\mathbf{d} \triangleq [\mathbf{d}_1^T, \mathbf{d}_2^T, \dots, \mathbf{d}_{M_S}^T]^T \in \mathbb{R}^{M \times 1}$ accounting for all per-subarray MA-positions $\{\mathbf{d}_s\}$. Given any optimized subarray-positions \mathbf{q}^* , problem (P2) reduces to the following problem for optimizing MA-positions \mathbf{d}

$$\begin{aligned} (P4) \quad \max_{\mathbf{d}} \quad & \check{R}(\mathbf{q}^*, \mathbf{d}) \\ \text{s.t.} \quad & (3a), (3b), \end{aligned} \quad (18a)$$

where $\check{R}(\mathbf{q}^*, \mathbf{d}) \triangleq \check{R}(\mathbf{q}^*, \{\mathbf{d}_s\})$. Similar to problem (P3), this problem is also challenging to solve optimally due to its non-convexity. To tackle this difficulty, we also employ the PSO algorithm to find a high-quality solution to problem (P4); the framework of which is similar to that in Section III-B1. Specifically, at the beginning of the antenna-wise PSO algorithm, a swarm of \check{I}_P (whose index set is denoted by $\check{\mathcal{I}}_P \triangleq \{1, \dots, \check{I}_P\}$) feasible position vectors are generated, each denoted by $\mathbf{d}_i^{(0)} \in \mathbb{R}^{M \times 1}, i \in \check{\mathcal{I}}_P$, with $\check{\mathbf{s}}_i^{(0)} \in \mathbb{R}^{M \times 1}, i \in \check{\mathcal{I}}_P$ denoting its initial speed. Then, a customized fitness function $\mathcal{F}_A(\mathbf{d})$ is designed as follows to evaluate the quality of an arbitrary MA-position \mathbf{d}

$$\mathcal{F}_A(\mathbf{d}) = \check{R}(\mathbf{q}^*, \mathbf{d}) - \kappa P_A(\mathbf{d}), \quad (19)$$

where the first term corresponds to the objective function of problem (P4) and $\kappa P_A(\mathbf{d})$ is the antenna-wise penalty function introduced to account for constraints (3a) and (3b). Specifically, $P_A(\mathbf{d})$ is given by

$$\begin{aligned} P_A(\mathbf{d}) = & \sum_{s=1}^{M_S} \sum_{a=1}^{M_A} \left(\left[d_{s,a} - \left(L_A - \frac{\lambda}{4} \right) \right]^+ + \left[\frac{\lambda}{4} - d_{s,a} \right]^+ \right) \\ & + \sum_{s=1}^{M_S} \sum_{a=1}^{M_A-1} \left[\frac{\lambda}{2} - (d_{s,a+1} - d_{s,a}) \right]^+. \end{aligned} \quad (20)$$

Note that the first term in (20) penalizes the constraint (3a) and the second term accounts for half-wavelength antenna-spacing constraint (3b).

Based on the designed fitness function \mathcal{F}_A in (21), the per-subarray MA-positions $\mathbf{d}_i^{(t)}$ can be updated in a similar manner to that in (17) (see Section III-B1). Let \mathbf{d}^* denote the suboptimal solution to problem (P4), which is obtained after \check{I}_T iterations. By alternately optimizing \mathbf{q} and $\{\mathbf{d}_s\}$ (equivalently \mathbf{d}) until convergence, a suboptimal solution to problem (P2) can be obtained.

Remark 1 (Algorithm convergence and computational complexity). Since the objective function of problem (P2) is non-decreasing over each PSO iteration (and thus over

Table I: Simulation parameters

Parameter	Value	Parameter	Value	Parameter	Value
f_c	10 GHz	$\frac{P_t \varpi^2}{\sigma^2}$	9.78 dB	L	24λ
M_S	4	L_A	$\alpha \frac{L}{M_S}$	α	$\frac{3}{8}$
κ	10^6	c_1, c_2	2	ω	0.9
$I_P = \check{I}_P$	300	$I_T = \check{I}_T$	200	N_{PA}	3

each AO iteration), the convergence of proposed AO-based PSO algorithm is guaranteed [9]. Next, the computational complexities of the proposed PSO algorithm for optimizing subarray-positions \mathbf{q} and MA-positions $\{\mathbf{d}_s\}$ are in the orders of $\mathcal{O}(I_P I_T)$ and $\mathcal{O}(\check{I}_P \check{I}_T)$, respectively. In addition, the complexity of MMSE receive beamforming is $\mathcal{O}(M^3)$. As such, the overall complexity of the proposed AO-based PSO algorithm is $\mathcal{O}((I_P I_T + \check{I}_P \check{I}_T) M^3 I_A)$, where I_A is the number of AO iterations.

IV. NUMERICAL RESULTS

In this section, we evaluate the performance of our proposed TL-MA architecture and AO-based PSO algorithm. Specifically, a TL-MA based BS equipped with $M = 12$ antennas serves $K = 3$ users. We assume that the spatial angles of all users follow $\theta_{k,n} \sim \mathcal{U}(-0.5, 0.5)$ rad and their path gains are set as $\beta_{k,n} \sim \mathcal{CN}(0, \frac{\varpi^2}{N_{PA}})$, with ϖ being the average power [7]. Moreover, the array length of each subarray is set as $L_A = \frac{\alpha L}{M_S}$, where $\alpha \in (\frac{M \lambda}{2L}, 1)$ is a parameter controlling the allowable region of per-subarray movement. It is worth noting that the array-wise MA architecture in [11] is a *special case* of the proposed TL-MA architecture with $\alpha = \frac{M \lambda}{2L}$ (i.e., 1/4 in this case). Unless otherwise specified, other parameters are set as Table I. For performance comparison, the following benchmark schemes are considered: 1) the element-wise SL-MA scheme in [9]; 2) the array-wise scheme in [11] (i.e., TL-MA w/ $\alpha = \frac{1}{4}$); and 3) the conventional FPA scheme.

In Fig. 2, we show the system sum-rate versus the number of subarrays M_S . Several key observations are made as follows. First, all the MA-based schemes achieve significant sum-rate improvement over the conventional FPA scheme, thanks to the additional DoFs introduced by position adjustment. Second, compared with the array-wise scheme, the proposed TL-MA scheme with different subarray lengths achieves better sum-rate performance. This is because the array-wise scheme adjusts large-scale movement only, while the TL-MA scheme can further fine-tune the positions of MAs, thereby offering more spatial DoFs. Third, increasing the number of subarrays (i.e., M_S) can improve the sum-rate performance when M_S is small. However, it may incur a slight rate loss when M_S is sufficiently large (i.e., $M_S \geq 3$ for $\alpha = 3/4$ in Fig. 2). This is expected since for the latter case, a large number of subarrays reduces the spatial DoFs available for small-scale fine-tuning (especially when α is large), although it can increase the DoFs in large-scale movement. This phenomenon reveals an inherent trade-off between large-scale and small-scale movements in the proposed TL-MA scheme.

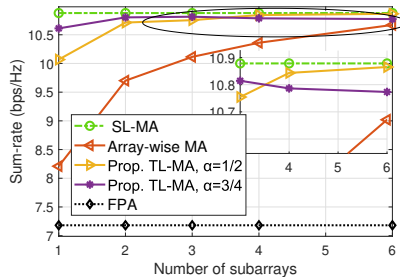


Fig. 2: Sum-rate vs. number of subarrays M_S .

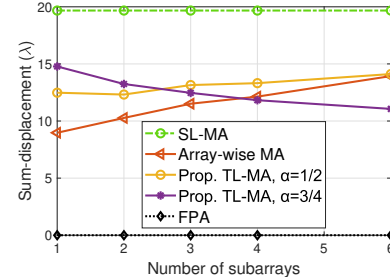


Fig. 3: Sum-displacement vs. number of subarrays M_S .

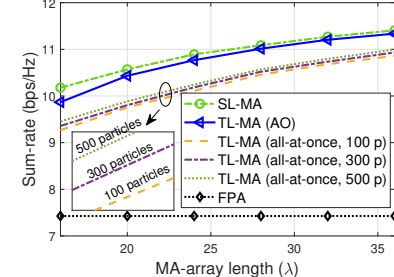


Fig. 4: Sum-rate vs. MA-array length L (100 p: $I_P = 100$).

In addition, we present the sum-displacement versus the number of subarrays M_S in Fig. 3. First, it is observed that although the SL-MA scheme achieves the highest sum-rate, it also incurs a significantly larger sum-displacement. In contrast, the proposed TL-MA architecture efficiently reduces the sum-displacement, while maintaining comparable rate performance with the SL-MA. Second, the TL-MA with different values of α exhibits different sum-displacement trends as M_S increases. Specifically, a larger α (e.g., $\alpha = \frac{3}{4}$) yields a larger fine-tuning movable region for MAs, making it the dominant contributor to the sum-displacement. The fine-tuning region (i.e., the length of each subarray) decreases as M_S increases, thus leading to a decreasing sum-displacement trend. In contrast, when α is small (e.g., $\alpha = \frac{1}{2}$ or $\frac{1}{4}$), the movable region for fine-tuning is limited, making the large-scale movement the main contributor. In this regime, the increasing trend of sum-displacement is expected since more subarrays introduce more large-scale movement. As such, for small subarray length architecture, decreasing M_S lowers sum-displacement but degrades rate; while for large subarray length architecture, increasing M_S is helpful for reducing sum-displacement but may reduce rate when M_S is large (see Fig. 2 for rate performance).

Last, in Fig. 4, we compare the sum-rates of different schemes versus MA-array length L . When the MA-array length increases from 16λ to 24λ , all MA-based schemes achieve increased sum-rates because the enlarged movable region enhances the spatial DoFs. Second, the proposed AO-based PSO algorithm achieves superior rate performance over the all-at-once PSO algorithm, even when the latter is associated more PSO particles. This is because in the all-at-once scheme, all variables (i.e., subarray-positions and MA-positions) are simultaneously optimized, which not only enlarges the dimensionality of variables, but also introduces complicated position constraints (see constraints (2)–(3)) that are coupled with variables, making the particle exploration more difficult. In contrast, the proposed AO-based PSO algorithm alternately optimizes the subarray-positions and MA-positions, reducing the dimensionality of each subproblem and decoupling the constraints from variables, thus facilitating the particle exploration.

V. CONCLUSIONS

In this letter, we proposed a new TL-MA architecture where the movement of each MA is decomposed into the

large-scale movement of subarrays and small-scale movement of per-subarray MAs. We formulated an optimization problem to maximize the uplink sum-rate. To solve this highly non-convex problem, we proposed an AO-based PSO algorithm, where the subarray positions and MA positions are optimized iteratively, given the optimal receive beamforming. Numerical results validated that the proposed TL-MA architecture significantly reduces the sum-displacement of SL-MA, thus alleviating the control complexity and hardware cost, while achieving comparable rate performance.

REFERENCES

- [1] C. You, Y. Cai, Y. Liu, M. Di Renzo, T. M. Duman, A. Yener, and A. Lee Swindlehurst, “Next generation advanced transceiver technologies for 6G and beyond,” *IEEE J. Sel. Areas Commun.*, vol. 43, no. 3, pp. 582–627, Mar. 2025.
- [2] K.-K. Wong, A. Shojaeifard, K.-F. Tong, and Y. Zhang, “Fluid antenna systems,” *IEEE Trans. Wireless Commun.*, vol. 20, no. 3, pp. 1950–1962, Nov. 2021.
- [3] W. Mei, X. Wei, B. Ning, Z. Chen, and R. Zhang, “Movable-antenna position optimization: A graph-based approach,” *IEEE Wireless Commun. Lett.*, vol. 13, no. 7, pp. 1853–1857, Apr. 2024.
- [4] X. Shao, W. Mei, C. You, Q. Wu, B. Zheng, C.-X. Wang, J. Li, R. Zhang, R. Schober, L. Zhu, W. Zhuang, and X. Shen, “A tutorial on six-dimensional movable antenna for 6G networks: Synergizing positionable and rotatable antennas,” *IEEE Commun. Surv. Tutor.*, 2025, Early Access.
- [5] B. Zheng, Q. Wu, T. Ma, and R. Zhang, “Rotatable antenna enabled wireless communication: Modeling and optimization,” *arXiv preprint arXiv:2501.02595*, 2025.
- [6] Z. Ding, R. Schober, and H. Vincent Poor, “Flexible-antenna systems: A pinching-antenna perspective,” *IEEE Trans. Commun.*, 2025, Early Access.
- [7] L. Zhu, W. Ma, W. Mei, Y. Zeng, Q. Wu, B. Ning, Z. Xiao, X. Shao, J. Zhang, and R. Zhang, “A tutorial on movable antennas for wireless networks,” *IEEE Commun. Surv. Tutor.*, 2025, Early Access.
- [8] W. Ma, L. Zhu, and R. Zhang, “MIMO capacity characterization for movable antenna systems,” *IEEE Trans. Wireless Commun.*, vol. 23, no. 4, pp. 3392–3407, Sep. 2024.
- [9] Z. Xiao, X. Pi, L. Zhu, X.-G. Xia, and R. Zhang, “Multiuser communications with movable-antenna base station: Joint antenna positioning, receive combining, and power control,” *IEEE Trans. Wireless Commun.*, vol. 23, no. 12, pp. 19 744–19 759, Nov. 2024.
- [10] B. Ning, S. Yang, Y. Wu, P. Wang, W. Mei, C. Yuen, and E. Björnsson, “Movable antenna-enhanced wireless communications: General architectures and implementation methods,” *IEEE Wireless Commun.*, 2025, Early Access.
- [11] H. Lu, Y. Zeng, S. Jin, and R. Zhang, “Group movable antenna with flexible sparsity: Joint array position and sparsity optimization,” *IEEE Wireless Commun. Lett.*, vol. 13, no. 12, pp. 3573–3577, Oct. 2024.
- [12] B. Lyu, C. Zhou, S. Gong, D. T. Hoang, and Y.-C. Liang, “Robust secure transmission for active RIS enabled symbiotic radio multicast communications,” *IEEE Trans. Wireless Commun.*, vol. 22, no. 12, pp. 8766–8780, Apr. 2023.